CONF-910864--14

UMassDHEP-E912

Presented at the 4th International Conference on Hadron Spectroscopy, Hadron '91, University of Maryland, College Park, 12-16 August 1991.

COMPARISON OF PWA RESULTS OF $K^+K^0{}_S\,\pi^-$ FINAL STATES PRODUCED IN 8 GeV/c K^-p, π^-p AND $\bar{p}p$ INTERACTIONS

Z. Bar-Yam 5), S. K. Blessing 3), A. Boehnlein 2), D. Boehnlein 2), B. E. Bonner 4), S U. Chung 1), J. M. Clement 4), R. R. Crittenden 3), J. Dowd 5), A. R. Dzierba 3), R. C. Fernow 1), J. H. Goldman 2), V. Hagopian 2), W. Kern 5), E. King 5) H. Kirk 1), N. Krishna 4), T. Marshall 3), G. S. Mutchler 4), D. C. Peaslee 1), S. D. Protopopescu 1), J. B. Roberts 4), P. Rulon 3 5), S. W. Teige 3), D. P. Weygand 1), H. J. Willutzki 1), D. Zieminska 3)

CONF-910864--14

Presented by J. Dowd

DE93 005215

1) Brookhaven National Laboratory, Upton, New York 11973, 2) Florida State University, Tallahassee, Florida 32306, 3) Indiana University, Bloomington, Indiana 47405, 4) Rice University, Houston, Texas 77251, 5) University of Massachusetts Dartmouth, North Dartmouth, Massachusetts 02747

ABSTRACT

We have performed partial-wave analyses of the $K^+K^0{}_S\,\pi^-$ system produced in the reactions $K^-p \rightarrow K^+K^0{}_S\,\pi^-\,\Lambda/\Sigma$, $\pi^-p \rightarrow K^+K^0{}_S\,\pi^-\,n$ and $\bar{p}\,p \rightarrow K^+K^0{}_S\,\pi^-\,X$ at 8 GeV/c in substantially the same apparatus. We present and compare the results of the analysis of the three reactions in the mass range 1.24 GeV/c^2 < M(KKπ) < 1.56 GeV/c^2. In all three reactions the $J^{PG} = 0^{-+}$, 1^{+-} and 1^{++} waves are the most important. A strong $f_1(1285)$ signal is evident in the π and $\bar{p}$ beam data sets but not in the K data. There is evidence of $\eta(1280)$ production, especially in the π and $\bar{p}$ beam data. We find evidence of two 0^{-+} states in the 1400 MeV/c^2 mass region, but no compelling case for a 1^{++} resonance in this region. Finally, the 1^{+-} wave in the K beam data is consistent with an h' state below the K^*K threshold.

Introduction

We report the results of a partial-wave analysis (pwa) of the $K^+K^0{}_S\pi^-$ system produced in the semi-inclusive reaction $K^-p \rightarrow K^+K^0{}_S\,\pi^-\,\Lambda/\Sigma$ at 8 GeV/c and compare the results with those of the pwa analyses of the exclusive reaction $\pi^-p \rightarrow K^+K^0{}_S\,\pi^-\,n$ and the inclusive reaction $\bar{p}\,p \rightarrow K^+K^0{}_S\,\pi^-\,X$ at 8 GeV/c. All three data sets were taken with the MPS-II spectrometer at Brookhaven National Laboratory as part of a comprehensive study of the production of $K^+K^0{}_S\,\pi^-$ states [1,2,3]. Partial wave fits to the π^- beam data [3] have been published and a mass dependent fit to the partial wave results has been reported at a previous conference [4]. The K beam and $\bar{p}$ beam data are described in recent conference reports and in theses [5,6].

A schematic view of the apparatus is shown in Fig. 1. Data with K and $\bar{p}$ beams were taken simultaneously in the AGS medium energy separated beam (MESB). The π^- data were taken earlier in the same beam in three separate runs. For all three beams the MPS facility was operated with a field of 0.5 tesla and a complement of 7 drift chamber modules, totalling 49 measuring planes, and 3 proportional chambers that were used in the triggering. A large high pressure segmented threshold Cerenkov counter (C1) located downstream of the MPS distinguished pions from heavier particles for momenta above 1.5 GeV/c. Three scintillation counter hodoscopes including a time-of-flight hodoscope were located downstream of C1. In the case of the π^- beam data only, the target was partially enclosed by a lead/scintillator sandwich veto counter.

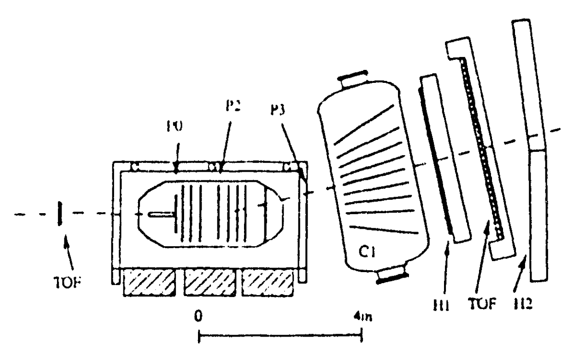

FIG. 1. MPS apparatus configured for E771

For all three data sets the trigger consisted of (i) a good beam particle requirement, (ii) a fast forward positive particle (FFP) requirement satisfied by a downstream particle heavier than a pion (i. e. a K^+ candidate), and (iii) a multiplicity (MULT) trigger to

MASTER

DISTRIBUTION OF THIS DOCUMENT IS UNLIMITED

FG05 87ER 40319

DISCLAIMER

This report was prepared as an account of work sponsored by an agency of the United States Government. Neither the United States Government nor any agency thereof, nor any of their employees, makes any warranty, express or implied, or assumes any legal liability or responsibility for the accuracy, completeness, or usefulness of any information, apparatus, product, or process disclosed, or represents that its use would not infringe privately owned rights. Reference herein to any specific commercial product, process, or service by trade name, trademark, manufacturer, or otherwise does not necessarily constitute or imply its endorsement, recommendation, or favoring by the United States Government or any agency thereof. The views and opinions of authors expressed herein do not necessarily state or reflect those of the United States Government or any agency thereof.

enhance the sample of $K^0{}_S$ decays. The FFP requirement was fulfilled by downstream particles that struck preselected combinations of PWC wires and hodoscope elements stored in a fast RAM memory. The combinations corresponded to the trajectories of positive particles of momenta greater than 1.5 GeV/c originating in the 60 cm hydrogen target. In addition the FFP trigger component required that the appropriate cell of the segmented Cerenkov counter C1 not fire.

The MULT trigger requirement was somewhat different in the three data sets. In the K and $\bar{p}$ beam data taking we required 2, 3 or 4 hits in proportional chamber P0 and 4 or 5 hits in chamber P2. For π^- data taking we required 2 hits in proportional chamber P0 and 4 hits in chamber P2. We also required that there be no signal in the target veto box for the π data.

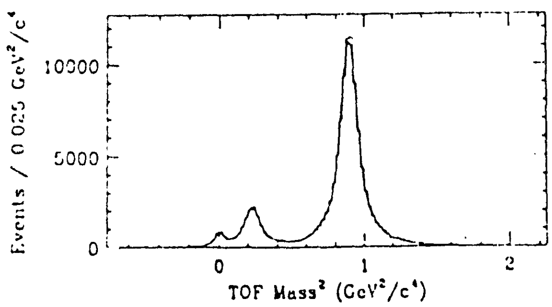

FIG. 2. TOF mass squared, fit with 5 Gaussians.

region	center value	width (GeV^2/c^4)
pion	0.0047±0.0012	0.0252±0.0012
kaon	0.2276+0.0007	0.0455±0.0011
		0.2020±0.0063
proton	0.8965±0.0003	0.0516±0.0007
		0.1466±0.0022

The high resolution time-of-flight system (σ = 150 ps) consisting of a 4-element hodoscope located upstream of the hydrogen target and a 32-element downstream hodoscope was used in the K/$\bar{p}$ run to separate kaons from protons off line (0.0 < $m_K{}^2$< 0.5 GeV^2/c^4). This was especially important in the case of the K data where the majority of the triggers were produced by downstream protons rather than by charged kaons. The TOF spectrum for the K beam data is shown in Fig. 2. The small admixture of pions seen in the TOF spectrum are at very low momentum and were removed by a momentum cut.

K^- Beam Data Set

A raw data sample of approximately 10^7 triggers was obtained with an exposure of 15 picobarn^{-1}. The data processing required that the events pass several stages of analysis. In the first stage, hits in the detectors were converted to real space coordinates, associated into tracks and assigned the measured three momenta and positions. A reconstructed beam particle, a K^+ candidate, at least one vertex, and at least 4 tracks were also required. Approximately 30% of the events survived this stage of processing.

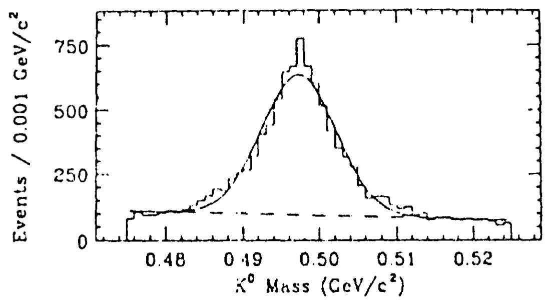

FIG. 3. K^0 mass spectrum, Gaussian fit: 427.29±0.08, σ =4.88±0.10 MeV/c^2.

A second stage required that a decay vertex consistent with the $K^0{}_S$ mass (0.475 < $m_{\pi\pi}$ < 0.525 GeV/c^2, see Fig. 3) be at least 2 cm downstream of the production vertex, and that the K^+ candidate, the $K^0{}_S$ and a negative track be on the production vertex. It also required that there be sufficient TOF information to calculate a mass for the K^+ candidate. Approximately 150,000 events passed this stage. The final processing stage required a positive identification of the K^+ by the TOF. The $K^0{}_S$ mass cut was narrowed (0.475 < $m_{\pi\pi}$ < 0.525 GeV/c^2). We required the K^+ candidate to be incompatible with the decay $\phi \to K^+ K^-$, and we also excluded $K^0{}_S$ candidates that satisfied a Λ decay hypothesis. A total of 9285 events survived all cuts and were written on the data summary tapes.

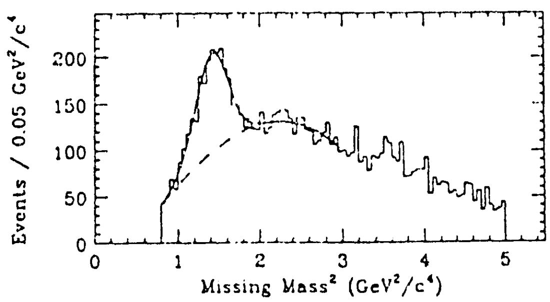

FIG. 4. Missing mass squared spectrum, Gaussian fit: 1.415±0.014, σ= 0.197±0.022 GeV^2/c^4, cubic background = 63% in the region of the mass cut.

A sample of 2700 events consistent with the semi-inclusive reaction $K^-p \rightarrow K^+K^0_S\,\pi^-\,\Lambda/\Sigma$ were selected by requiring the missing mass squared to be between 0.8 GeV^2/c^4 and 1.8 GeV^2/c^4 and -t to be < 1.4 GeV^2/c^2. The missing mass squared spectrum is shown in Fig. 4. The raw $K^+K^0_S\,\pi^-$ mass spectrum of these events plotted in 10 MeV bins is shown in Fig. 5b and the corresponding acceptance corrected spectrum in Fig. 5c. It is to be emphasized that this spectrum is corrected for phase space only --- it is not the result of a PWA fit. The shape of the spectrum is similar to that reported by LASS [7] for the same reaction at 11 GeV/c and by Ph. Gavillet et al. [8] at 4.2 GeV/c. The $K^+K^0_S\,\pi^-$ mass spectrum shows a strong enhancement at the threshold for K^*K production at 1390 MeV/c^2. There are relatively few events in the 1280 MeV/c^2 mass region. In the region near 1530 GeV/c^2 there is only a hint of an enhancement in the raw data.

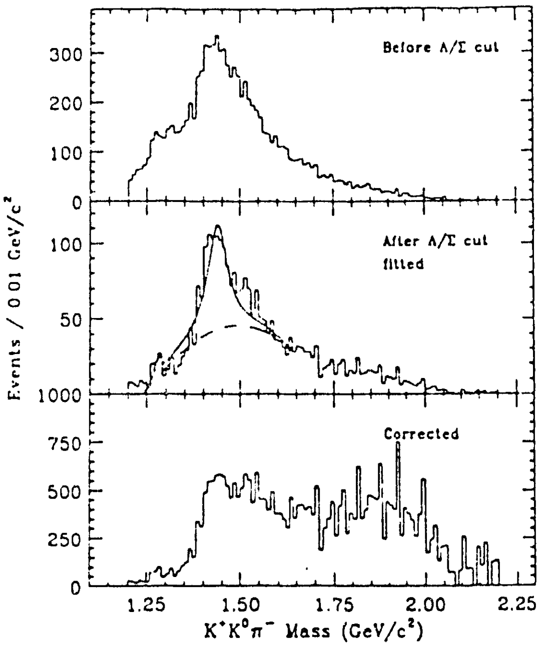

FIG. 5. $K^+K^0_S\,\pi^-$ mass spectrum, fit: two Breit-Wigners plus polynomial.

central value	width (GeV/c^2)	events
1.280±0.001	0.012±0.012	22±7
1.438±0.003	0.063±0.003	262±17

A partial wave analysis of this data was performed. The $KK\pi$ system was described as a superposition of states characterized by spin, parity, and G parity, J^{PG}, the projection of spin on the quantization axis, M (≥ 0), and reflectivity (naturality of the exchanged particle), η. We applied the parametrization of the spin-density matrix of Chung and Trueman [9] which ensures that the conditions of positivity, parity conservation, and rank 2 are automatically satisfied with the minimum number of parameters.

We assumed that the final three-meson system is produced in a two-step process involving two isobars: $K^*(890)$ and $a_0(980)$. For a given $KK\pi$ mass and a given -t, the state is fully specified by five variables: the isobar mass and the polar and azimuthal angles for the primary and secondary decays. We also allowed for an incoherent isotropic background. A PWA program written specifically for this experiment was used. This program uses the extended maximum-likelihood method and includes the effect of finite acceptance in the normalization integrals.

J^{PG}	M	η	isobar	mass range (GeV)
0^{-+}	0	+	a_0	all
1^{++}	0	+	K^*	mass > 1.34
1^{++}	1	+	K^*	mass > 1.46
1^{++}	1	-	K^*	mass > 1.46
1^{+-}	0	+	K^*	1.34 < mass< 1.54
1^{+-}	1	+	K^*	1.34 < mass< 1.54
1^{-+}	0	-	K^*	mass > 1.46

TABLE 1. Partial waves used in fit

In this fit to the data the waves $J^{PG} = 0^{-+}, 1^{++}, 1^{+-}$ and 1^{-+} were found to be important in various regions of $K^+K^0_S\,\pi^-$ mass. For each wave in each mass region not all possible combinations of isobar, M and η were found to be significant. For example, the $J^{PG} = 0^{-+}$ wave in the K^*K channel was found to

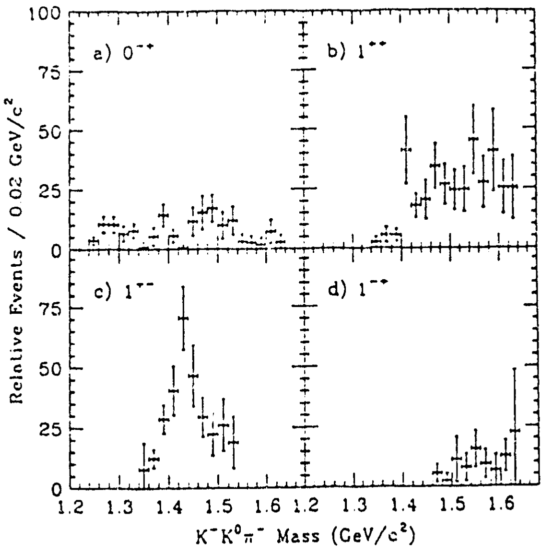

FIG. 6. Relative number of events for the J^{PG} partial waves used in the pwa fit summed over M and η.

be small and only the decay channel $a_0(980)$ is present in this fit. For $J^{PG} = 1^{++}$ we found that the contribution of $a_0(980)$ to the fit was small. The waves used in the fit are summarized in Table 1. In addition an incoherent isotropic background was used in the fit. The analysis was carried out on 2043 events in 20 MeV bins over the mass range 1.24 - 1.64 GeV/c^2. The relative number of events in the four J^{PG} partial waves used are shown in Fig. 6.

In the 1.28 GeV/c^2 mass region we see some evidence for a small $J^{PG} = 0^{-+}$ $\eta(1280)$ contribution, while the 1^{++} wave was small enough to be turned off. There is no evidence for the $f_1(1285)$ in the K beam data set.

We observe a large enhancement of events at the threshold of K^*K production. Above this threshold in the 1400 Mev/c^2 mass region the $J^{PG} = 1^{+-}$ and 1^{++} waves dominate with the 1^{+-}wave the most important in the 1420 - 1460 MeV/c^2 mass region. The $J^{PG} = 0^{-+}$ partial wave is also present.

The relative number of events in the large $J^{PG} = 1^{+-}0^{+}$ and $1^{+-}1^{+}$ partial waves that are most important in the 1400 MeV/c^2 mass region are shown in Fig.7. The $1^{+-}1^{-}$ wave was found to be small and is turned off in the fit. Fig. 8 shows the relative magnitude square of the complex $1^{+-}0^{+}$ and $1^{+-}1^{+}$ amplitudes. From this figure we see that the $1^{+-}0^{+}$ is stronger than the $1^{+-}1^{+}$. Finally the shape of the magnitude squared of the complex

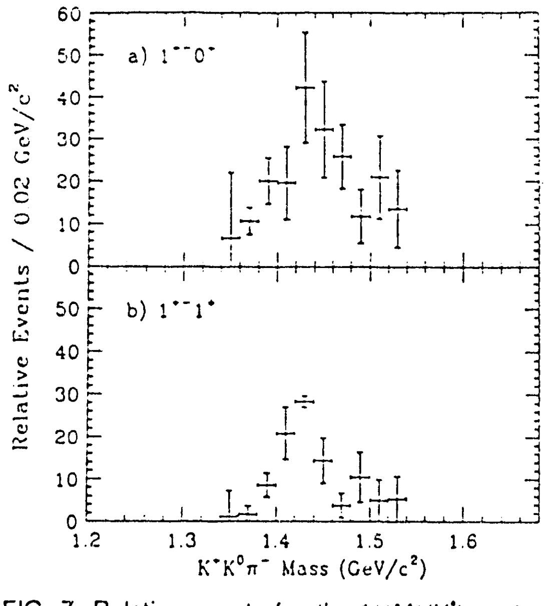

FIG. 7. Relative events for the $1^{++}M^{+}(K^*)$ partial waves.

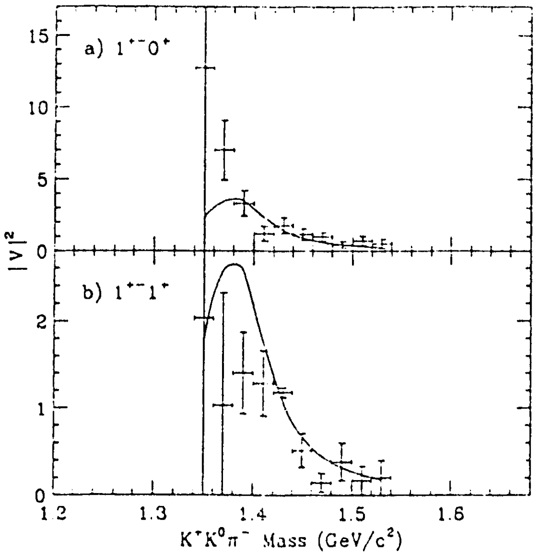

FIG. 8. Combined fit with LASS [7] parameters: central value = 1380±20, Γ = 80±30 GeV/c^2.

amplitudes is consistent with a $J^{PG} = 1^{+-}$ h' resonance existing below the K^*K threshold. A similar threshold behavior of the 1^{+-} partial wave has been reported by the LASS [7] group. The solid curve in Fig. 8 is a combined fit to both M^{η} waves in our data using the parameters reported by the LASS group.

The magnitudes squared of the J^{PG} $M^{\eta} = 1^{++}0^{+}$,

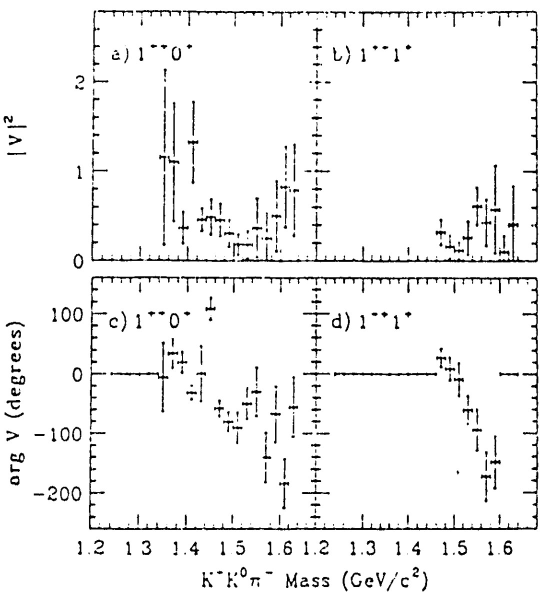

FIG. 9. Magnitude squared and phase of the fit parameters for the $1^{++}M^{+}(K^*)$ partial waves.

and $1^{++}1^{+}$ partial waves are shown in Figs. 9a and 9b, and their phase variation relative to the $0^{-+}\ 0^{+}$ (a_0) partial wave in Figs. 9c and 9d. The generally decreasing phase of the 1^{++} partial waves may be interpreted as evidence supporting resonance behavior in the 0^{-+} wave in the 1400 MeV/c^2 mass region. In the region around 1530 MeV/c^2, the 1^{++} partial wave intensity shows no obvious indication of the $f_1(1530)$ reported by LASS. This may be related to the semi-inclusive nature of our measurement. An earlier LASS partial wave analysis [10] of inclusive $KK\pi$ production also found no evidence of a resonant 1^{++} wave in this mass region.

The $J^{PG} = 0^{-+}$ (a_0) partial wave is relatively weak but the shape of the wave is consistent with two resonances in this mass region. The low bin at 1430 Mev/c^2 has persisted throughout many fits.

Comparison to π^- Beam Data Set

A raw data sample of approximately 9×10^6 triggers was obtained with an exposure of 1 picobarn^{-1} in an 8 GeV/c π^- beam. The data processing imposed cuts similar to those in the K beam data, except that the TOF requirement was not used for this data. Approximately 52,000 events passed the cuts and were written to the data summary tapes. A final sample of 27,481 events with $1.24 \le M(KK\pi) \le 1.56$ GeV/c^2 and $0.0 \le -t \le 1.0$ GeV^2/c^4 was used for further analysis.

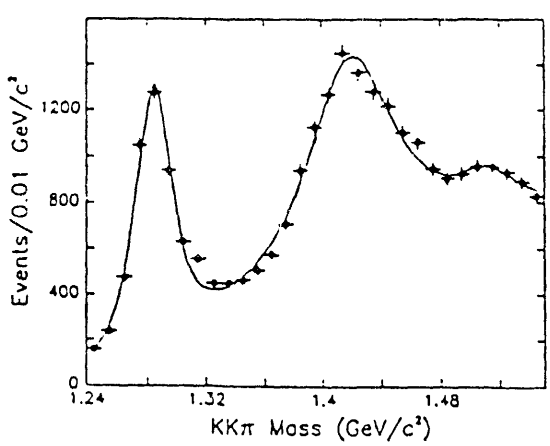

FIG. 10. $K^+K^0_S\pi^-$ mass spectrum, fit: three Breit-Wigners plus polynomial.

central value	width (GeV/c^2)
1.285±0.001	0.022±0.002
1.419±0.001	0.066±0.002
1.512±0.004	0.035±0.015

The $K^+K^0_S\pi^-$ mass spectrum of these events plotted in 10 MeV bins is shown in Fig. 10. The spectrum shows a similar strong enhancement at the threshold for K^*K production at 1390 MeV/c^2 as the K beam data. In contrast to the K data there is a large peak in the 1280 MeV/c^2 mass region. In the region near 1530 MeV/c^2 there is some indication of an enhancement in the raw data.

The partial wave analysis of the π beam data used $J^{PG} = 0^{-+}$, $1^{++}, 1^{+-}$, 1^{--}, and 1^{-+} waves for all possible values of M^{η} for both ($a_0\pi$) and (K^*K) decay channels in 20 MeV bins in the mass range 1.24 - 1.56 GeV/c^2. However below the K^*K threshold the $1^{++}(a_0)$ and the 1^{++} (K^*) waves were not distinguishable, while above the threshold the $1^{++}(a_0)$ was small. In the fit we allowed only $1^{++}(a_0)$ for $M(KK\pi) < 1.34$ GeV/c^2 and only $1^{++}(K^*)$ above 1.34 GeV/c^2.

The spin-parity components summed over M, η, and isobar for the three most important waves, $J^{PG} = 0^{-+}$, 1^{++}, and 1^{+-} are shown in Fig. 11. In the 1280 MeV/c^2 mass region there is a prominent peak that is dominated by the 1^{++} wave. The 1^{++} wave is essentially absent in this mass region in our K data. This is consistent with little or no $s\bar{s}$ content in the $f_1(1285)$. The π beam data also show an indication of a peak in the $0^{-+}(a_0)$ wave in this mass region, consistent with the presence of the $\eta(1280)$.

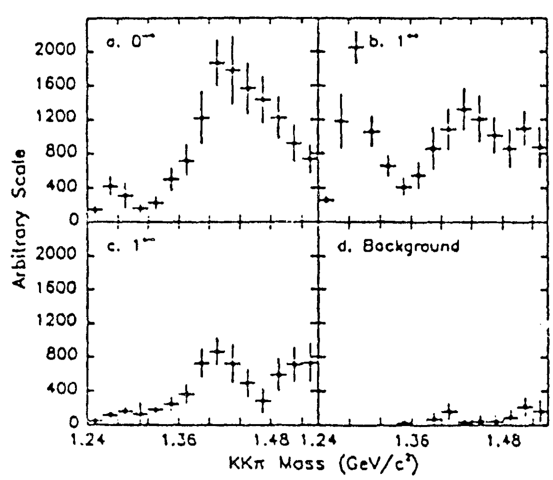

FIG. 11. Relative events in the major spin-parity components.

In the 1400 MeV/c^2 mass region the $J^{PG} = 0^{-+}$ wave is the most important wave, followed by the

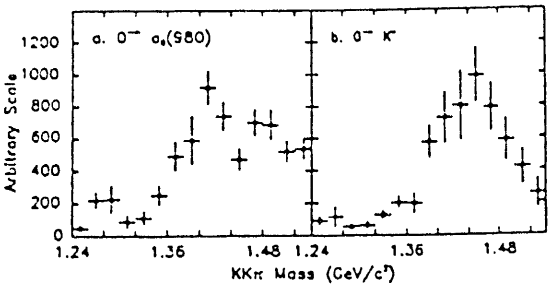

FIG. 12. Relative events in the $0^{-+}(a_0)$ and $0^{-+}(K^*)$ waves.

1^{++} and the 1^{+-} waves. This is exactly the opposite order of relative importance in the K beam data. Fig. 12 shows the $0^{-+}(a_0)$ and the $0^{-+}(K^*)$ contributions separately. Both decay modes are important, and the K^* contribution appears to peak at a higher $KK\pi$ mass than that of the a_0. A measurement of the coherence (not shown) between these two partial waves shows that they are strongly coherent below about 1.38 GeV/c^2 and relatively incoherent in the 1400 MeV/c^2 mass region. In addition the phase of the $1^{++}0^{+}(K^*)$ with respect to the $0^{-+}(a_0)$ shows a rapid fall in this region, especially for four momentum transfer $-t \geq 0.2$ GeV^2/c^2. Taken together this evidence suggests the existence of two 0^{-+} states in this mass region.

A series of mass dependent fits of the PWA results at the level of the production amplitudes was made simultaneously in three separate four-momentum transfer regions to our high statistics π beam data. In the fits the incoherent part of the $0^{-+}(K^*)$ wave was parameterized by a single Breit-Wigner in the 1400 MeV/c^2 mass region. In the PWA, the phase of the $1^{++}0^{+}(K^*)$ with respect to the $0^{-+}(a_0)$ at $-t \leq 0.2$ GeV/c^2 in the 1400 MeV/c^2 mass region is relatively flat, indicating a possible resonance at low t in the 1^{++} partial wave. However the mass dependent fits are also consistent with a nonresonant behavior of this partial wave. The most economical fit (a combination of fits B and E of reference 4) would require a $0^{-+}(a_0)$ $\eta(1280)$, and two 0^{-+} resonances in the 1400 MeV/c^2 mass region - one decaying primarily to $(a_0\pi)$, and a second one decaying to (KK^*). Despite the relatively large contribution of the 1^{++} wave, only one 1^{++} resonance is mandatory, a $f_1(1285)$. Attempts to include the important 1^{+-} wave in the mass dependent fit gave inconsistent results, and the final fit was made to the 0^{-+} and 1^{++} waves only. The parameters of the fit are given in table 2.

J^{PG}	Mass	Width (MeV/c^2)
$0^{-+}(a_0)$	1312±3	29±6
$0^{-+}(a_0)$	1407±3	75±6
$0^{-+}(K^*)$incoherent	1405±10	135±1
$1^{++}(a_0)$	1299±1	30±6

TABLE 2. Summary of fit parameters.

Comparison to $\bar{p}$ Beam Data Set

A raw data sample of approximately 5.2×10^6 triggers corresponding to an exposure of 12 pb^{-1} was obtained for the inclusive reaction $\bar{p}\,p \to K^+K^0_s\,\pi^-\,X$ at 8 GeV/c. Processing cuts were similar to those used in the K beam data, including a TOF mass identification of the downstream K^+. No missing mass cut was made. A total of 3595 events with $1.24 \leq M(KK\pi) \leq 1.56$ GeV/c^2 and $-0.2 \leq -t \leq 1.2$ GeV^2/c^2 were used in the PWA.

The $K^+K^0_s\pi^-$ raw mass spectrum of the $\bar{p}$ beam data (see Fig. 13) is similar to the π beam data -- it exhibits a strong peak in the 1280 MeV/c^2 mass region and a broad peak in the 1400 MeV/c^2 mass region -- but there is no hint of a peak in the 1500 MeV/c^2 mass region.

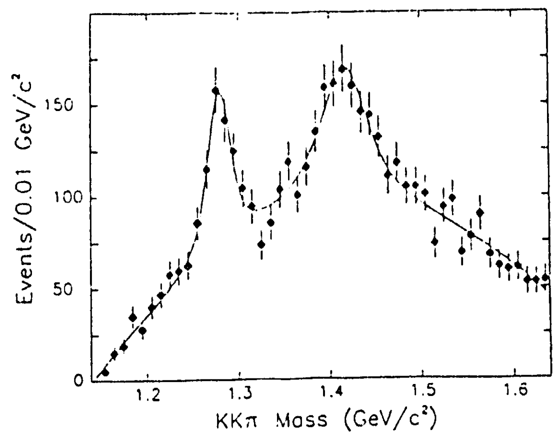

FIG. 13. $K^+K^0_s\,\pi^-$ mass spectrum, fit: two Breit-Wigners plus polynomial.

central value	width (GeV/c^2)
1.279±0.002	0.021±0.002
1.417±0.003	0.062±0.005

The partial wave analysis of the $\bar{p}$ beam data used $J^{PG} = 0^{-+}(a_0$ and $K^*)$, 1^{++}, (a_0 and K^*) and 1^{+-} (K^*) waves in 20 MeV bins. As in the case of the π and K beam fits, we allowed only $1^{++}(a_0)$ for $M(KK\pi) <$ 1.34 GeV/c^2 and only $1^{++}(K^*)$ above this mass. The 1^{+-} wave is relatively small in this data set but it is needed to fit the K^{*-}/K^{*0} asymmetry (not shown) above 1400 MeV/c^2. Allowing all M^η combinations for the 1^{+-} waves resulted in two different solutions for the pwa fit that differed in the relative amounts of 1^{++} and 0^{-+} waves in the three mass bins between 1.38 and 1.44 GeV/c^2. The ambiguity was removed by turning off the relatively unimportant $1^{+-}0^+$ and $1^{+-}1^-$ waves. In the final fit, the $1^{+-}1^+$ was also turned off below 1.34 GeV/c^2.

The spin-parity components for the final fit are shown in Fig. 14. In the 1280 MeV/c^2 mass region peaking is seen in both the $0^{-+}(a_0)$ and the 1^{++} waves. The phase motion (not shown) of the $0^{-+}(a_0)$ with respect to the $1^{++}0^+(a_0)$ in this mass region is relatively flat -- consistent with the presence of a resonance in both waves. As in the π beam data the 0^{-+} wave is the most important wave above the K^*K threshold, and as in both the π and K beam cases the 1^{++} also shows a strong enhancement above the K^*K threshold. The $0^{-+}(a_0)$ shows a strong positive phase motion relative

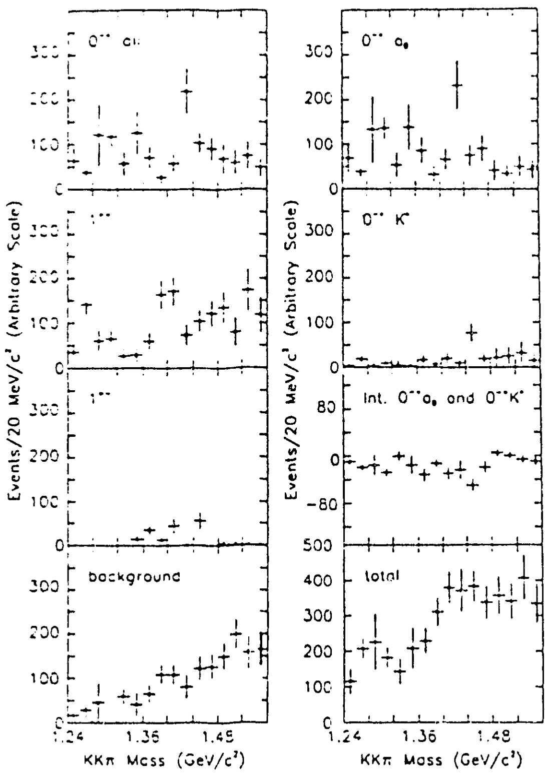

FIG. 14. Spin-parity components in pwa fit to $\bar{p}$ data.

to the $1^{++}0^+K^*$ in this region (see Fig. 15) indicating that the 1^{++} wave, while relatively large, may not be resonating. The $0^{-+}(K^*)$ is very small throughout the mass range with only the single bin centered at 1.45 GeV/c^2 substantially above zero.

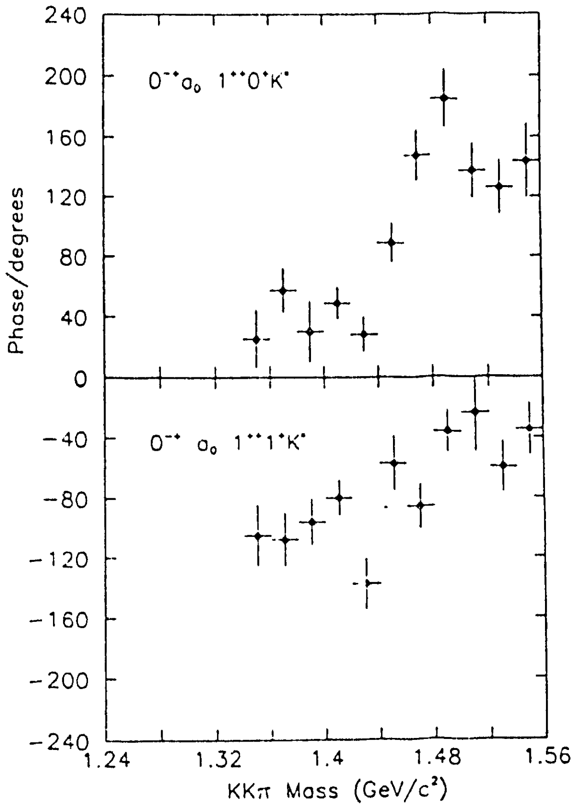

FIG. 15. Phase of $0^{-+}(a_0)$ with respect to $1^{++}(K^*)$.

The fit to the $\bar{p}$ beam data set is very similar to the π beam pwa fit. The most obvious difference is the relative lack of $0^{-+}(K^*)$ in the 1400 MeV/c^2 mass region as compared to the π beam data set where this was an important partial wave. In addition the $f_1(1285)$ is stronger in the π data than in the $\bar{p}$ set, and the $\bar{p}$ data shows no indication of structure in the 1500 MeV/c^2 mass region.

Summary

In the 1280 MeV/c^2 mass region the $f_1(1285)$ contributes most strongly in the π data, and is also prominent in the $\bar{p}$ data, while it is absent from the K data. This is consistent with the behavior of a state that is mainly not $s\bar{s}$. The $J^{PG} = 0^{-+}$ $\eta(1280)$ is required in the fits to all three data sets, but it is weak in all of them, especially the K data set.

The situation in the mass region above 1400 MeV/c^2 is not so straight forward. Three waves, 0^{-+}, 1^{++}, and 1^{+-}, are present in all three data sets with varying relative importance. There is evidence in our high statistics π data for two 0^{-+} states in this region - one decaying primarily via ($a_0\pi$) and the other decaying primarily by (K^*K). Our K data shows an indication of two peaks in the $0^{-+}(a_0)$ wave in this

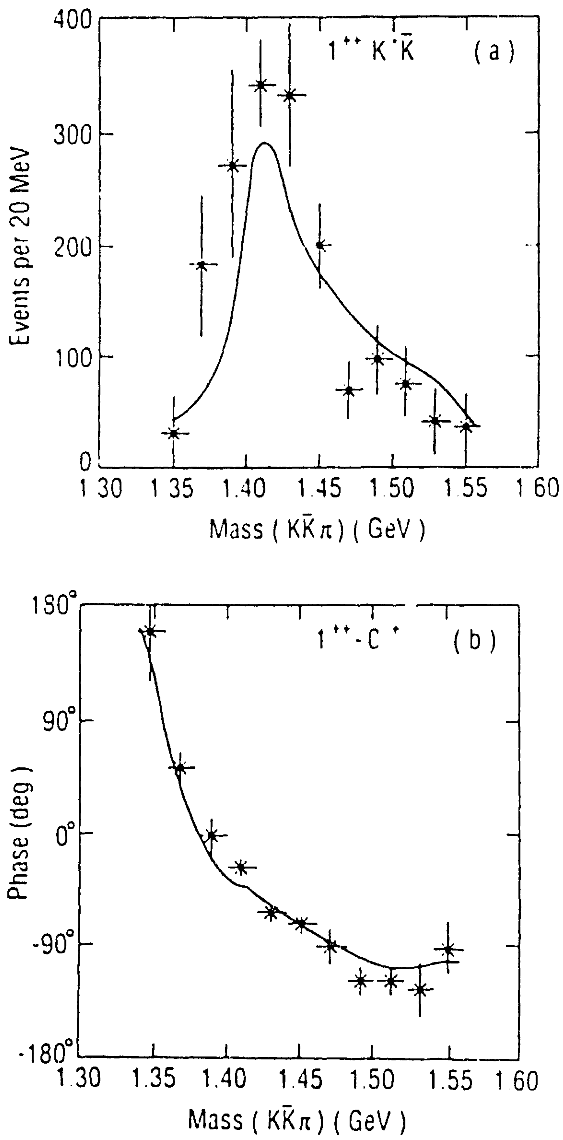

FIG. 16. $K\bar{K}\pi$ molecular model fit to the intensity (FIG. 16a.) and phase (FIG. 16b.) of the 1^{++} partial wave in the E771 π data. See Longacre [12].

mass region. In the K data only the ($a_0\pi$) decay mode was significant for the 0^{-+} wave. The fit to the $\bar{p}$ data requires a large $0^{-+}(a_0)$ contribution but very little $0^{-+}(K^*)$. Recent data from MKIII [11] in J/ψ radiative decay also supports the presence of two 0^{-+} resonances in this region. They report a 0^{-+} ($a_0\pi$) at 1416 MeV/c^2 and a $0^{-+}(K^*K)$ at 1490 MeV/c^2.

The 1^{+-} wave is also present in all three data sets, but it is the dominant wave only in the K beam data. In our data we see strong evidence for a below threshold h' state. The parameters of this state are consistent with those reported by the LASS group.

The 1^{++} wave is important in all three data sets above the K^*K threshold, but the phase motion of this wave is not strong in any of the data sets. A possible explanation of this puzzling behavior has recently been suggested by Longacre [12]. He proposes a $K\bar{K}\pi$ molecular model for the 1^{++} state, and uses the model to fit our intensity distribution for the 1^{++} wave and its phase variation. The fit (shown in Fig. 16) is impressive.

References

[1] S.U. Chung et al., Phys. Rev. Lett. 55 (1985) 779.

[2] D. Reeves et al., Phys. Rev. D34 (1986) 1960.

[3] A. Birman et al., Phys. Rev. Lett. 61 (1988) 1557.

[4] π data: S. Blessing et al., Proceedings of *Glueballs, Hybrids, and Exotic Hadrons*, Upton, NY, 1988 (AIP Conf. Proc. No. 185) 363; S. Blessing, thesis, Indiana Univ. (1988), unpublished.

[5] K data: E. King et al., Nucl. Phys. B21 (1991) 11; E. King, thesis U. Mass. (1991), unpublished.

[6] $\bar{p}$ data: A. Boehnlein et al., Nucl. Phys. B21 (1991) 142; A. Boehnlein, thesis, Florida State Univ. (1991), unpublished.

[7] D. Aston et al., Phys. Lett. B201 (1988) 573.

[8] Ph. Gavillet et al., Z. Phys. C16, (1982) 119.

[9] S. U. Chung and T. L. Trueman, Phys. Rev. D11 (1975) 633.

[10] D. Aston et al., Phys. Rev D32 (1985) 2255.

[11] Z. Bai et al., Phys.Rev. Lett. 65 (1990) 2507.

[12] R. S. Longacre, Phys. Rev. D42 (1990) 874.

END

DATE
FILMED

2 /23/ 93